

Performances and Limitations of Wind Speed Sensor Equalization

Felipe Miguel Aparicio Acosta

Laboratoire de Traitement des Signaux
Ecole Polytechnique Fédérale de Lausanne
CH-1015 Lausanne Suisse
email: aparicio@ltssun2.epfl.ch

Résumé

Cet article discute les problèmes liés à l'égalisation de la réponse dynamique des anémomètres, et en particulier celle des *anémomètres à moulinet*. Des modèles non-linéaires à multi-phase sont proposés pour corriger certains comportements non-linéaires de ce type de capteurs. Leurs performances et leurs limitations sont illustrées et discutées par la suite.

1 Introduction

Cup anemomenters are part of the classical instrumentation used for obtaining measurements of wind speed and direction, and usually designed to monitor only characteristics of horizontal air flow. They are simple, sturdy and only require a modicum of maintenance, which make them suitable for operation under extreme meteorological conditions (i.e. strong winds). However, their response may be far from ideal mainly due to either faulty calibration, *off-axis response*, nonzero *starting threshold* and *overspeeding*.

The problem of faulty calibration is that the small residual differences between the tunnel wind speed and the rate of rotation of the anemometer may be severely amplified in a turbulent flow. The off-axis response is the ratio of the measured wind speed at different angles of attack to the measured wind speed at zero angle of attack. The starting threshold is the lowest wind speed at which a rotating anemometer starts turning and producing a measurable signal, and ideally, should be zero. Finally, overspeeding is caused by the nonlinear response of these anemometers to fluctuating winds, which is faster for an increase than for a decrease in wind speed of equal magnitude. Friction in the bearings and inertia are the sources of these two latter nonlinearities.

Abstract

In this paper we discuss the problem of equalizing the nonlinear dynamic response of some wind speed sensors, in particular the so called *cup anemometers*. We propose piecewise nonlinear models to correct some of the nonlinearities typical in these sensors and thus control their response. The performances and limitations of one such a model will be illustrated on real wind speed data.

2 Calibration of Cup Anemometers

The rate of rotation of the cups is adjusted in a steady laminar wind produced at a wind tunnel [1]. The calibration equation for a cup anemometer can be easily derived from its equation of motion:

$$I * d\Omega/dt = T(v_1, v_2, r\Omega) - T_f \quad (1)$$

where I denotes the moment of inertia, r the cup-arm radius, T is the torque exerted by the wind field on the instrument, v_1 and v_2 are respectively the horizontal and vertical components of the wind speed, and T_f is the frictional torque produced at the bearings.

It has been suggested on geometrical grounds that:

$$T(v_1, v_2, r\Omega) = \alpha v_1^2 f(r\Omega/v_1, v_2/v_1); \quad (2)$$

where α depends on the dimensional and geometrical parameters of the anemometer and of the density of the air.

Now, a linear approximation of $f(\cdot)$ and a quadratic approximation for T_f such as $T_f \approx a_1 v_1 + a_2 v_1^2$ yields a linear calibration function after making $T(v_1, v_2, r\Omega) = T_f$:

$$v_1 = v_a + cr\Omega \quad (3)$$

where $c = (c_0 - a_2/\beta\alpha)$ is called the *calibration factor*, c_0 is the calibration factor for the frictionless case, and $v_a = a_1/(\beta\alpha - a_2)$ is called the *apparent starting*



speed, which differs in general from the starting threshold. Both c and v_a depend on the cup-wheel geometry through the parameter β . In practice, the linear calibration formula is only valid for values of v_1 higher than a starting threshold v_s .

3 Dynamical Behaviour

Calibration in the wind tunnel according to equation (3) is not enough to control the dynamic behaviour of a cup anemometer when exposed to fluctuating winds. The dynamic response of a cup anemometer can be studied by integrating the first order nonlinear differential equation which results from replacing the torque $T(\cdot)$ with its Taylor series expansion around an equilibrium point $(v_{10}, v_{20}, \Omega_0)$. We can express the solution of this equation as:

$$\Omega_t = g(\mathbf{v}_t, \theta), \quad (\mathbf{v}_{t0}, \Omega_{t0}) = (v_{10}, v_{20}, \Omega_0) \quad (4)$$

where θ is a parameter vector encoding the physical characteristics of the anemometer. The first-order component in the Taylor series expansion for the torque $T(\cdot)$ can explain the linear dependencies between Ω_t and \mathbf{v}_t , and the damping of the high-frequency fluctuations. But the asymmetry of the response to these fluctuations can only result from higher-order components. This asymmetry manifests itself in the different time of response of the anemometer for increasing and decreasing steps in wind amplitude. The latter phenomena, known as *overspeeding*, causes an overestimation of the mean wind speed measured in turbulent flow if the sensor was calibrated in laminar flow. The nonlinear nature of this overestimation, which distinguishes it from being due to faulty calibration, shows itself in its dependency with respect to the turbulence intensity. Indeed, it can be shown [2] that the relative overspeeding about the mean value of the horizontal wind speed v_{10} can be approximated by:

$$\Delta\Omega/v_{10} \approx (\sigma_{v_1}^2/v_{10}^2)J; \quad (5)$$

where J is a monotonically increasing function of the weight and dimensions of the anemometer, and $\sigma_{v_1}^2$ denotes the variance of the horizontal wind speed component. The first factor on the right is the square of the *turbulence intensity*, defined as σ_{v_1}/v_{10} .

4 Anemometer Equalization

Equalizing the dynamic response of an anemometer is not an easy task. First, since we do not know the true wind flow \mathbf{v}_t , we may think of using the response of a

sophisticated anemometer with high performances as a reference. However, it is not possible to establish an absolute reference for all atmospheric conditions and for all responses, since any anemometer is subject to its own limitations. Fortunately, these limitations are often different in nature and therefore we may use the responses of sensors behaving differently under identical flow conditions in order to infer part of the dynamics of one sensor. This is called *transfer model building*, and one of its applications is to predict the behaviour of one instrument from a projection (generally, nonlinear) of its dynamics onto those of another instrument, which we suspect to perform poorly when subject to the same flow conditions. The transfer model establishes the way in which this projection is carried out, and has to be estimated with both sensors being synchronized and operating under identical conditions. The reference could be provided by any anemometer not exhibiting the particular feature which we want to correct in the response. The second and more crucial problem is that, even if a certain sensor seems to be appropriate as a reference for dealing with a particular feature, we have little guidance as to the suitability of this reference for different atmospheric conditions than those at which the model was established. Nevertheless, if the dynamics are well behaved with respect to varying turbulence conditions and assuming that proper compensations are provided for eventual drifts in atmospheric variables such as temperature, it may be possible to capture the evolution of the estimated transfer model for changing turbulence settings. For that, time records of the responses of the sensors are required for a sufficiently wide spectrum of flow conditions.

4.1 Problem Formulation

Let \mathbf{c}_t be the vector containing the time series of horizontal wind speed measurements provided by our cup anemometer, and let \mathbf{r}_t be that provided by an appropriate reference. Both sensors are assumed to be synchronized, and closely spaced so as to avoid any meaningful lag in the responses, but without causing mutual obstruction of the incoming air flow.

We are interested in inferring \mathbf{r}_t from \mathbf{c}_t , or equivalently, in compensating for the undesirable trends in \mathbf{c}_t , which we assume to be lacking in the reference \mathbf{r}_t . That is, we look for an equalizing transformation $h(\cdot)$ such that:

$$\mathbf{r}_t = h(\mathbf{c}_t) + \epsilon_t \quad (6)$$

where ϵ_t contains, ideally, a series of *i.i.d.* random variables. A first simplification comes from considering only zero-memory transformations $h(\cdot)$ such that $\mathbf{r}_t = h(\mathbf{c}_t) + \epsilon_t$. On the other hand, each time series can

be expressed in terms of a particular transformation of the underlying wind flow \mathbf{v}_t :

$$r_t = F(\mathbf{v}_t, \theta_r) \quad (7)$$

$$c_t = F(\mathbf{v}_t, \theta_c) \quad (8)$$

The parameter vector θ embodies, on the one hand, the dimensions, geometry and other physical constraints of the sensor, as well as the characteristic constants of the signal conditioning circuitry in the translator, and, on the other hand, the dependencies of the anemometer performances on external variables (i.e. temperature, humidity, etc).

Our aim is to estimate the functional form of the conditional expectation $\mathcal{E}[r_t | c_t]$, and to do that we remark that the function $F(\mathbf{v}_t, \theta_r)$ can be expanded in a Taylor series around the point θ_c in parameter space:

$$F(\mathbf{v}_t, \theta_r) = F(\mathbf{v}_t, \theta_c) + (\theta_r - \theta_c)' \left(\frac{\partial F(\mathbf{v}_t, \theta)}{\partial \theta} \right)_{\theta_c} + \dots \quad (9)$$

The first partial derivative of $F(.,.)$ appearing in the previous equation measures the sensivity of the response with respect to changes in the parameters about those values for which there is perfect matching between the outputs of both sensors. All derivatives can be regarded as the parameters of our model, and our task consists in estimating their functional forms.

If we assume that the parameter mismatches are small enough so that we can neglect higher-order derivatives, the coarsest equalization we may think about is given by:

$$F(\mathbf{v}_t, \theta_r) = F(\mathbf{v}_t, \theta_c) + (\theta_r - \theta_c)' \mathbf{C} \quad (10)$$

where \mathbf{C} is a vector constant. This model is unsatisfactory in practice, and a more sensible assumption would be that the first partial derivative of $F(.,.)$ be proportional to $F(\mathbf{v}_t, \theta_c)$. This is realistic as far as the overspeeding is concerned, since the amount of overestimation in the mean wind speed tends to be larger for strong gusts. Although this preliminary model can explain the overestimation in mean wind speed caused by the overspeeding phenomena, it may not be able to forecast its evolution for different turbulence statistics. A better approximation will account for the dependency of \mathbf{C} with respect to the turbulence intensity, which, according to (5), is linear to first order. Therefore we may write:

$$\mathbf{C} = \mathbf{C}_0 \frac{\sigma_c^2}{\mathcal{E}[c]} \quad (11)$$

where \mathbf{C}_0 is a vector constant, and σ_c^2 is the variance of the horizontal wind speed measured by the cup anemometer about the mean value $\mathcal{E}[r]$. Our experimental plots show that the overestimation for given

turbulent conditions does not obey to a linear dependence rule with regards to all (horizontal) wind speed amplitudes. Indeed, the linear fit for medium to large amplitudes cannot always be extrapolated to the range of small amplitudes, and a piecewise linear or polynomial fit seems more appropriate. For that we only need to consider for \mathbf{C}_0 a non-constant value of the type

$$\mathbf{C}_0 = 1 + b_1 F(\mathbf{v}_t, \theta_c) + b_2 (F(\mathbf{v}_t, \theta_c))^2 + \dots \quad (12)$$

for a polynomial fit. Another possibility would be to split our model into a piecewise linear fit:

$$F(\mathbf{v}_t, \theta_r) = F(\mathbf{v}_t, \theta_c) + C_{00} \sigma_{v_1}^2 (\theta_r - \theta_c)' F(\mathbf{v}_t, \theta_c) \quad (13)$$

for $F(\mathbf{v}_t, \theta_c) > t_c$, and

$$F(\mathbf{v}_t, \theta_r) = F(\mathbf{v}_t, \theta_c) + C_{01} \sigma_{v_1}^2 (\theta_r - \theta_c)' F(\mathbf{v}_t, \theta_c) \quad (14)$$

for $F(\mathbf{v}_t, \theta_c) \leq t_c$, and where C_{00} and C_{01} are scalar constants.

In any case, the previous models only apply for those readings beyond a starting threshold, which can be estimated by isolating those time instants at which the cup anemometer measurements vanish but not the reference's. The most important limitations of these models arises from the implicit dependence of $(\theta_r - \theta_c)$ on variables which are exogenous to the anemometer, such as temperature, and also from the dependence of $F(.,.)$ on the flow characteristics through \mathbf{v}_t , one aspect of which is the turbulence intensity. These dependences impair the forecasting ability of the model, and thereby the equalization performances obtained when used to control the anemometer dynamics. A refinement of these models could be achieved by analyzing and modeling the way in which the wind speed readings of the two anemometers are affected by changes in the atmospheric conditions.

4.2 Results

In this section we illustrate the anemometer equalization problem on real data. The model was inferred from synchronized paired data obtained from a Sonic anemometer (used here as reference) and a nearby Lambrecht cup anemometer, and was used to equalize the readings of the latter at a different time period. The Sonic apparatus, which rely on the dependence of the transit time of a sonic pulse on the transmitting medium, was selected as a reference because of its avoidance of inertial sensing components. The data consisted of wind speed averages at every ten minutes, and was divided into two blocks corresponding to consecutive time periods. The second time period is characterized by the presence of a storm, which causes relatively large values for the averages as compared to



the scatter diagram of the Sonic data plotted against the Lambrecht's. The slope in this plot clearly differs from unity, which explains the mean wind speed overestimation. Figure 1.2, which plots the Sonic minus Lambrecht data against the Lambrecht's, reveals that the overestimation only shows up at speeds beyond a certain threshold. This nonlinearity was replicated in a bi-phase model [3], with a polynomial regime for small speed values, and a linear regime for medium to large speed values (figure 1.3). Figure 1.4 shows the residuals after detrending figure 1.2 with this model. Figure 2 corresponds to the second time period, which we use to test the previous model. As shown in figures 2.1 and 2.2, the range of speed values is larger than in the previous block. The forecasting ability of the model is shown in figure 2.4, where the residual trend observed at the end of the data reveals that the overestimation is likely to increase nonlinearly and faster for large speed values. But more data at this range of large amplitudes would be needed in order to infer properly this diverging behaviour from linearity. Finally, figure 3.1 shows clearly the overestimation of the mean wind speed in the Lambrecht data corresponding to an interesting interval of the second time period. The results after equalizing the Lambrecht readings with the model inferred from the first block of data are shown in figure 3.2. The standard deviation of the Sonic minus Lambrecht data, estimated for the whole second time period, drops from 0.2863 to 0.0862 after correction, which means a gain of 10.4dB. The previous model is only valid for wind speed values beyond the starting threshold, which was estimated to be around 0.3m/sec.

References

- [1] J.T. Snow, D.E. Lund, M.D. Conner, S.B. Hartley, and C.B. Pedigo. The dynamic response of a wind measuring system. *Journal of Atmospheric and Oceanic Technology*, 6:140–146, 1989.
- [2] F. Dobson, L. Hasse, and R. Davis. *Air-Sea Interaction: instruments and methods*. Plenum Press, 1980.
- [3] G. A. F. Seber. *Nonlinear Regression*. John Wiley and Sons, 1988.

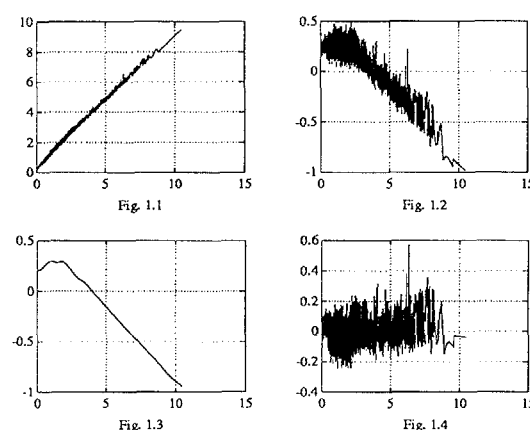


Figure 1: Inference of a two-regime model for anemometer equalization.

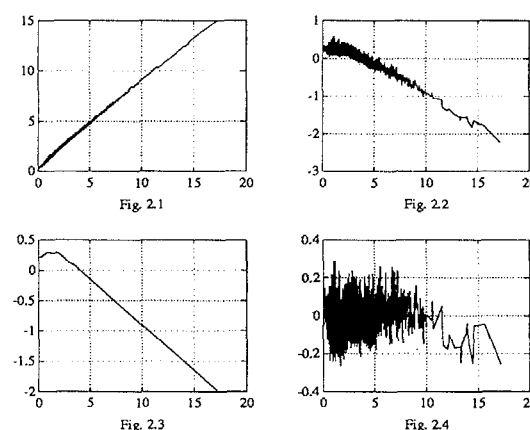


Figure 2: Model testing.

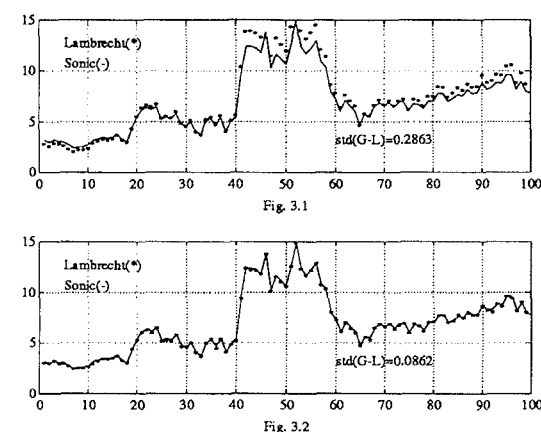


Figure 3: Comparison of wind speed data before and after equalization.